LA-UR-96- 1893

CONF-9609220--1

Title: A Comparison of Different Texture Analysis Techniques

Author(s): S. I. Wright, TexSEM Laboratories, Inc.
U. F. Kocks, CMS, LANL

Submitted to: Invited Keynote speaker at Eleventh International Conference on Textures of Materials
Xian, China
September 16-20, 1996

Los Alamos
NATIONAL LABORATORY

Form No. 836 R5
ST 2629 10/91

DISCLAIMER

A COMPARISON OF DIFFERENT TEXTURE ANALYSIS TECHNIQUES

S. I. Wright[1] and U. F. Kocks[2]

[1]TexSEM Laboratories, Inc., 226 West 2230 North #120, Provo, UT 84604 USA
[2]Center for Materials Science, Mail Stop K765, Los Alamos National Laboratory, Los Alamos, NM 87545 USA

ABSTRACT

With the advent of automated techniques for measuring individual crystallographic orientations using electron diffraction, there has been an increase in the use of local orientation measurements for measuring textures in polycrystalline materials. Several studies have focused on the number of single orientation measurements necessary to achieve the statistics of more conventional texture measurement techniques such as pole figure measurement using x-ray and neutron diffraction. This investigation considers this question but also is extended to consider the nature of the differences between textures measured using individual orientation measurments and those measured using x-ray diffraction.

Keywords: diffraction, texture

INTRODUCTION

Textures in polycrystalline materials have most commonly been determined using pole figure measurements obtained by x-ray diffraction. Many experimental and analytical methods have been developed for determining polycrystalline orientation distributions (often referred to as ODFs or ODs) using the pole figure technique. However, with the advances in electron diffraction techniques in recent times, it has become practical to measure textures using single orientation measurements obtained by electron diffraction.

Currently, the most common electron diffraction technique used for texture measurement is based on electron backscatter diffraction in the scanning electron microscope (SEM). When a beam of electrons of narrowly defined energy is focused onto a crystal lattice, an electron backscatter diffraction pattern (EBSP) can be formed on a detector (a phosphor screen) mounted in the SEM chamber. A high gain video camera transmits this image to a computer workstation. Image feature recognition techniques are then used to index the digitized EBSP to acquire the crystallographic orientation. The indexing of the EBSPs along with control of the electron beam in the SEM has been automated so that it has become feasible to obtain thousands of single orientation measurements in a matter of hours [1-2]. (The automated analysis of EBSPs is often termed orientation imaging microscopy or OIM.)

While both x-ray and electron diffraction provide the data necessary to characterize the distribution of orientation in a polycrystalline sample it should be noted that X-ray diffraction is an average measurement technique, whereas electron diffraction is a point-specific orientation measurement

technique. Electron diffraction allows local textures and point-to-point orientation relationships to be characterized. It also has the advantage that a complete description of the OD can be determined from the measurements. Classical pole figure techniques provide only incomplete OD information due to the absence of the so-called missing odd-l coefficients (see for example Matthies[3]). Numerical methods have been developed for indirectly resolving this ambiguity[4-5]. One drawback of the electron diffraction technique is the difficulty of obtaining reliable data from heavily strained materials. The presence of dislocations in the crystal lattice causes the diffraction patterns (in the SEM) to be more diffuse making it difficult to reliably obtain the orientation from an EBSP. The OIM technique is also limited to materials with grain sizes exceeding at least a tenth of a micron.

Bowen [6] has noted some possible sources for error in obtaining accurate measurements of texture using local orientation measurements. One possibility is that arises from errors in alignment of the specimen in the SEM. However, it should be noted that both techniques (x-ray and electron diffraction) are subject to alignment errors. Originally, textures measured using electron diffraction by measuring the orientations grain by grain in a polycrystal. Bowen pointed out that errors can be introduced into the calculation of the OD if the sizes of the grains are ignored. The electron diffraction measurements used in the work presented here were obtained using the OIM technique. In this technique, orientation measurements are made on regular hexagonal grids. Thus, large grains are sampled more often than small grains and a true area fraction is obtained.

The intent of this paper is to compare some specific textures obtained by electron diffraction with textures obtained from x-ray pole figures. Several papers have sought to define the number of measurements needed to accurately measure an OD using local orientation measurements with respect to an OD determined using x-ray pole figures[7-10]. Some of these papers have shown that while the two methods produce similar textures they do not converge to the same solution. While, this work will consider the question of how many measurements are needed to determine a statistically reliable OD, the primary focus will be to investigate the differences in textures measured by x-ray pole figures and textures measured using local orientations in detail relative to the locations of these differences in orientation space. Much of the data analysis presented in this paper was done using popLA (preferred orientation package - Los Alamos) [11].

To aid in the comparison of textures the following parameter will be used to characterize the overall difference between two ODs:

$$D_A^B = [\Sigma(f_A(g) - f_B(g))^2]^{1/2}/[\Sigma f_B(g)^2]^{1/2}, \quad (1)$$

where D_A^B is the overall difference between the ODs $f_A(g)$ and $f_B(g)$. The summation is performed over all points in the calculated OD. In this paper, the ODs were calculated on 5×5×5 degree grids in Euler space. In addition, "difference" pole figures and ODs will be used to compare different textures. A difference OD is calculated by subtracting one OD from another at each point of the grid in Euler space. Difference pole figures are generated in the same manner.

OIM VS. X-RAY TEXTURES

1. Forged copper

10,160 orientation measurements were made on a sample obtained from a forged cone of high-purity copper. The measurements were made on a 7mm×1mm hexagonal grid with 25μm spacing between measurement points. The average grain size was 60μm. (111), (200) and (220) pole figures were measured on a specimen of the same material using x-ray diffraction. The material exhibited a weak fiber texture near (110). Fig. 1 shows a comparison of the (110) pole figures generated from the x-ray

and OIM data. The differences in the pole figures are most prominent near the central peak, but are less than one times random.

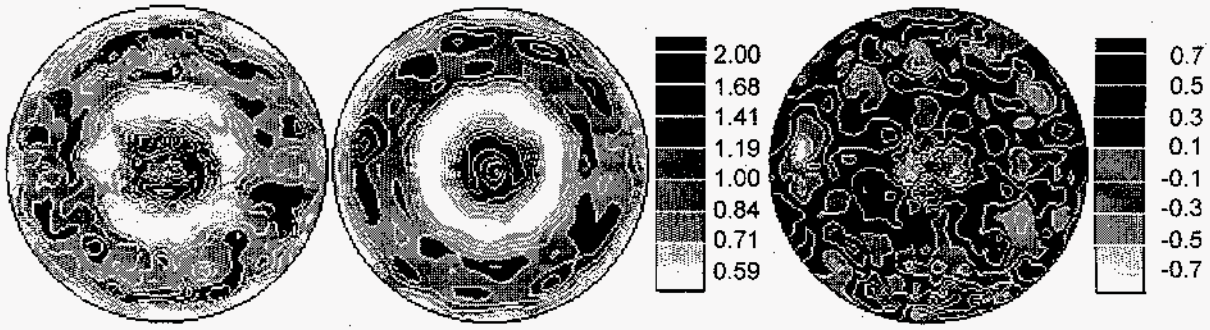

Fig. 1 (110) x-ray, OIM and difference pole figures for forged copper.

The OIM pole figure shown in Fig. 1 was generated by taking each of the individual orientation measurements in the OIM along with all of the symmetrically equivalent orientations (making use of the cubic crystal symmetry) and incrementing the appropriate bins in a 5x5x5 degree discretization of Euler space. This array is the normalized and then smoothed by convoluting the array with a Gaussian with a 5° half-width. The degree of smoothing applied to the OIM data will have an effect on the match between the resulting smoothed OIM OD and the x-ray OD [7-8]. The effect of smoothing is shown in Fig. 2. This plot was constructed by calculating smoothing the binned arrays with Gaussians of halfwidths, ω, ranging from 0° to 15° in step of 1°. D_ω^X was calculated at each ω, where the X denotes the x-ray OD and ω represents the smoothed OIM OD. For this data set, it appears that smoothing with an 8° Gaussian produces the best match between the OIM OD and the x-ray OD.

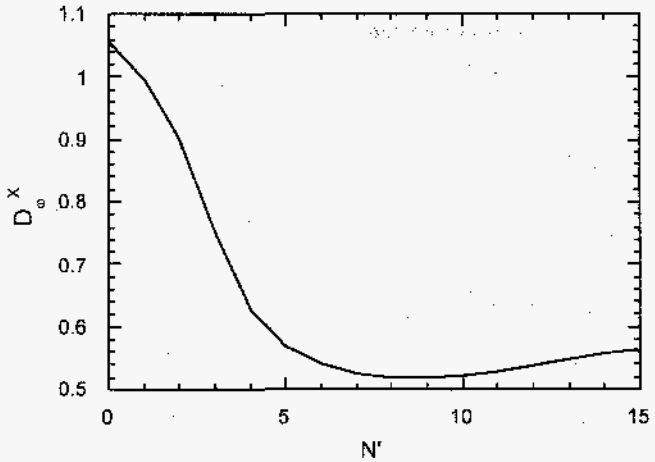

Fig. 2 Plot of D_ω^X versus ω. (X represents the x-ray OD and ω represents the OIM OD smoothed with a Gaussian of half-width ω.)

2. Rolled copper

16,723 orientation measurements were made on a sample of 58% cold-rolled OFE copper. The measurements were made on a 2.5mm×1mm hexagonal grid with 10μm spacing between measurement points. The average grain size was 52μm. (111), (200) and (220) pole figures were measured on a specimen of the same material using x-ray diffraction.

ODs generated for the OIM data and the x-ray data along with a difference OD are shown in Fig. 3. These ODs are presented in oblique sections through Euler space. The sections are constant ν section where $\nu = (\psi + \phi)/2$, where ψ, Θ, ϕ are Euler angles according to Kocks[12]. Oblique sections are used

to avoid the distortions in Euler space near $\Theta = 0$. The approximate location of the β and α fibers are overlaid on the difference OD in Fig. 3.

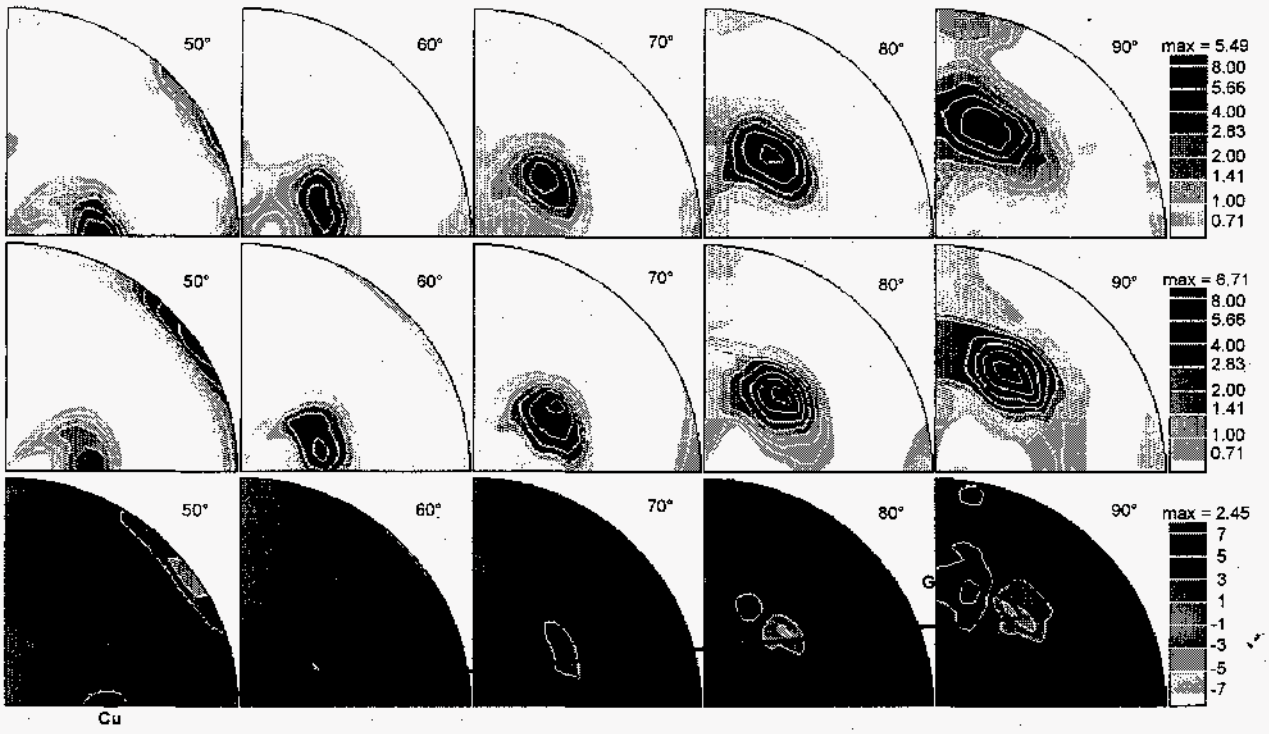

Fig. 3 X-ray, OIM and difference ODs plotted in oblique sections for rolled copper.

While the OIM ODs and x-ray ODs look quite similar, closer examination of the ODs shown in Fig. 4 shows that there is a shift away from the brass component towards the Goss component in the OIM OD relative to the x-ray OD. Yield surface predictions based on the OIM and x-ray ODs are slightly different[13]. The OIM data predicts greater sideways anisotropy than the x-ray data. In fact, mechanical tests of this material showed an even greater sideways anisotropy than that predicted by the OIM measurements. The parameter $D_O{}^X = 0.47$ for the ODs shown in Fig. 4 (the O denotes the OIM OD and X denotes the x-ray OD).

The x-ray measurement was taken from the center plane perpendicular to the normal direction of the sheet. The OIM measurements were obtained from the center section of a plane normal to the transverse direction of the sheet. While some surface to centerline texture gradients would be expected in the sheet, the textures obtained were from the centerline of the sheet which should minimize any texture gradient effects.

To get a sense of the magnitude of the differences observed between the x-ray and OIM ODs, ODs were calculated from the x-ray pole figure data using the WIMV and harmonic approaches as implemented in popLA. In these calculations, orthorhombic sample symmetry was enforced and the harmonic series expansion was carried out to $l = 22$. Recalculated (111) pole figures are shown in Fig. 4. It should be noted that for these calculations $D_H{}^W = 0.22$ (the H signifies the harmonic calculation and the W denotes the WIMV calculation).

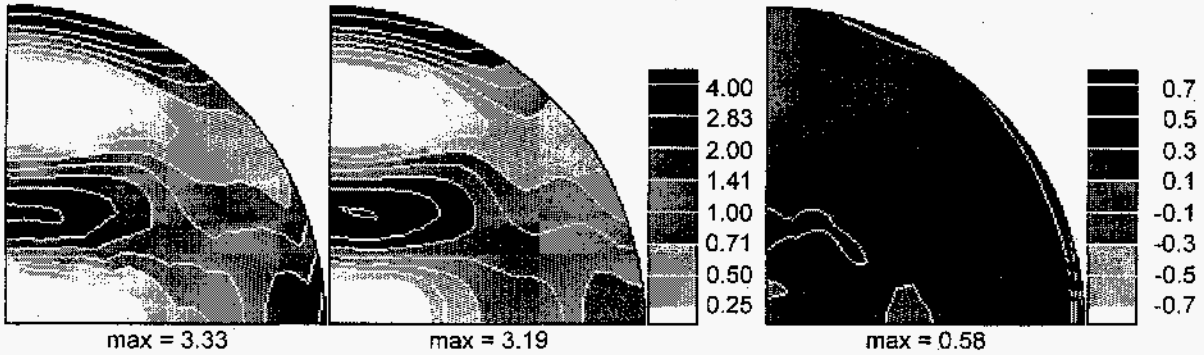

Fig. 4 Pole figures for x-ray data recalculated from ODs calculated using the WIMV method and the harmonic series expansion method along with a difference pole figure.

For each point in an OIM an image quality parameter (IQ) is recorded which describes the quality of the corresponding EBSP. Lower quality patterns are less likely to be correctly indexed by the automatic EBSP indexing software than higher quality patterns. Thus, the orientations obtained for low quality patterns may be less reliable than those obtained for high quality patterns. Low quality patterns are produced when the crystal lattice is distorted. In the case of this cold rolled material, the deformation distorts the crystal lattice degrading the patterns from deformed material. To examine the effect of image quality on the results, the OIM data for the rolled copper was partitioned into a set of points with IQs less than 4 (12% of the measurements) and a set of points with IQs greater than 4 (remaining 88%). ODs were then calculated for these two sets of data. The resulting ODs are shown in Fig. 5.

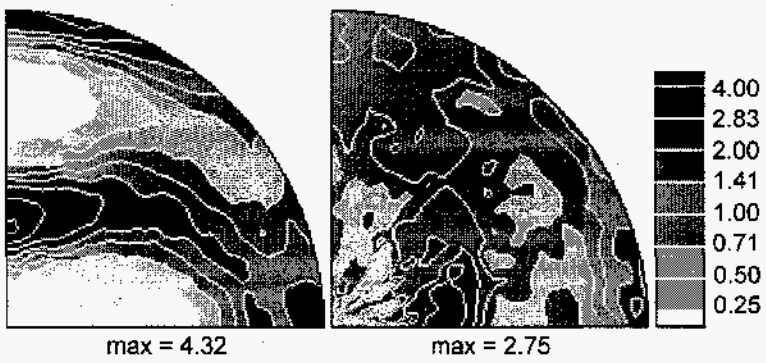

Fig. 5 (111) Pole figures using for OIM data with IQs greater than 4 and IQs less than 4.

Fig. 5 shows that the pole figure generated from the low IQ measurements is quite a bit different from the pole figure generated from the high IQ measurements. The low IQ OD is more random than that calculated for the high IQ measurements. The average IQs for the measurements within 15° of brass was 8.4 and for Goss was 7.6, the overall average IQ was 7.6. (IQs ranged from 3.1 to 49.0 in this scan.)

There is some indication that strain is not uniformly distributed in a deformed microstructure. There appears to be a preference for grains of particular orientations to strain more than grains of other orientations. Thus, in deformed materials some components may be underpredicted by OIM due the inability to obtain indexable EBSPs from grains of these preferentially strained grain orientations. X-ray and neutron diffraction are not susceptible to these problems arising from strain. Hollinshead [14] has observed an absence of the copper texture component in manually indexed EBSP measurements of texture in rolled aluminum compared to x-ray textures.

Just as there are different techniques available for reducing pole figure data to ODs, different techniques can be used to calculate textures from OIM data leading to discrepancies arising from the different data reduction methods used. Fig. 6 shows a (111) pole figure calculated using harmonic analysis and a pole figure calculated using the binning method described earlier. A difference pole figure is also shown. The

difference parameter D_H^B equals 0.31 for these two ODs (B denotes the OD calculated using the binning algorithm in popLA and H denotes an OD calculated using harmonics). The harmonics were calculated assuming a 5° Gaussian at each data point[7]. Fig. 6 suggests that more smoothing of the data occurs in the harmonic method than in the binning method. Some of additional smoothing is probably due to the truncation of the series expansion at $l = 22$.

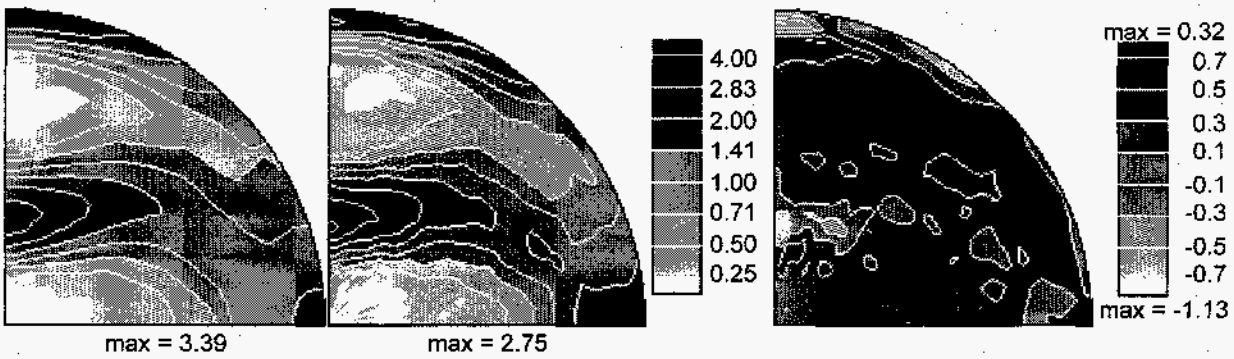

Fig. 6 (111) pole figures generated by the harmonic series expansion and the direct space method using the OIM data.

3. Cross-Rolled tantalum

11,428 orientation measurements were made on a cross-rolled (93% reduction) and annealed (at 1050°C for 1 hour) tantalum sample using OIM. The measurements were made on a 4mm×15mm hexagonal grid with 25μm spacing between measurement points. The average grain size was 136μm. (110), (200) and (111) pole figures were measured on a specimen of the same material using x-ray diffraction. The raw pole figure data along with an unsmoothed pole figure from the OIM data is shown in Fig. 7.

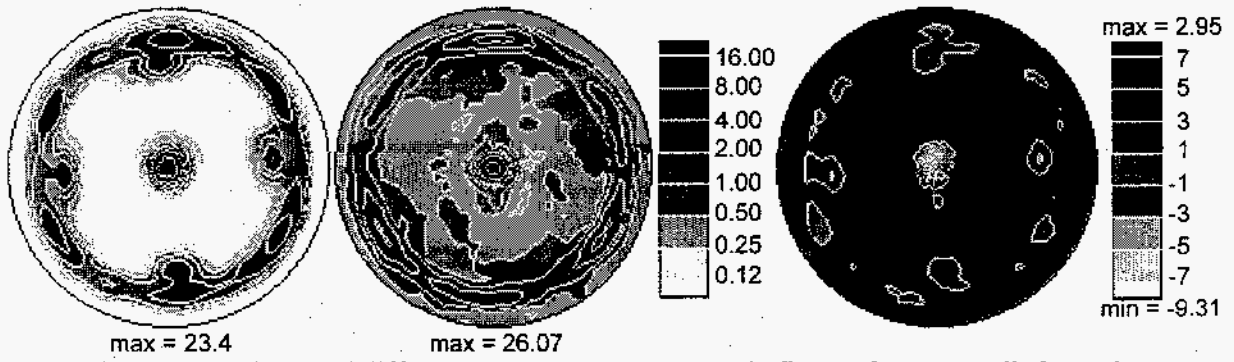

Fig. 7 X-ray, OIM and difference (OIM-x-ray) (111) pole figures for cross rolled tantalum

As observed in the forged copper example, the most prominent difference between the x-ray and OIM pole figures is near the central peak. While the peak heights are quite similar, the shapes of the peaks are quite different resulting in a difference in the pole figures exceeding nine times random. The other notable difference is the absence of the cube component in the OIM pole figure. The OIM measurements were made on a plane normal to the transverse direction of the rolled sheet, the x-ray measurements were made on a plane perpendicular to the normal direction of the sheet. Gradients in texture have been frequently observed in tantalum plate materials [15,16] - the surface of the plate often exhibits a stronger preference for cube oriented material than the centerline of the sheet. The sheet used in this example was 0.76 mm thick. The x-ray sample was prepared by mechanically grinding the sample to allow the texture from the center plane to be measured. However, with such a thin sample it is likely that some misalignment may have occurred during the grinding process resulting in material near the specimen surface being sampled in the pole figure measurement. This may account for the difference in increased cube component in the x-ray measured textures.

OIM TEXTURES

As stated earlier, several studies have addressed the question of how many single orientation measurements are needed to calculate a statistically reliable OD. These studies have generally concluded that approximately 1000 measurements are needed to accurately determine an OD. However, most of these papers have used only 1000 measurements to reach this conclusion. Using OIM, it is possible to measure tens of thousands of measurements with relative ease. Thus, these studies have been replicated with many more measurements to provide a clearer understanding of the statistical sampling question.

In order to investigate this question, the data from four separate OIM scans were used. Summary information for these scans is given in the following table.

Table 1 Summary information for OIM scans

Data Label	avg. grain diameter	no. measurements	no. grains	scan width	scan height
Fiber Al	0.35	35,436	7082	40μm	31μm
Rolled Al	76	27,384	2765	7mm	6mm
HIP Ta	21	10,360	3947	1mm	1mm
Ta Plate	136	11,428	1065	0.4mm	15mm

The data labeled *Fiber Al* was obtained from an Al-0.5 weight %Cu sample formed by chemical vapor deposition. This sample exhibited a strong (111) fiber texture. The *Rolled Al* data was obtained from a 40% channel-die compressed sample of commercially pure aluminum. This sample exhibited a moderate rolling texture. The *HIP Ta* data was obtained from a tantalum powder metallurgy sample that was hot isostatically pressed at 1400-1800°C at 207MPa. This sample displayed a nearly random texture. The *Ta Plate* sample is the cross-rolled tantalum sample described previously.

$D_{N'}^{N}$ was calculated for each of the scans for N' ranging from 100 to N in steps of 100. N is the total number of measurements in a scan and N' represents a subset of the measurements contained in a scan containing N' measurements. Results for the four scans are shown in Fig. 8.

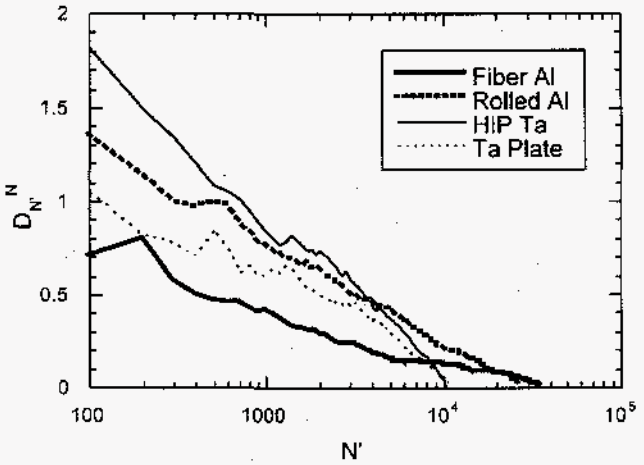

Fig 8. Plot of $D_{N'}^{N}$ versus N'.

As would be expected, as N' approaches N, $D_{N'}^{N}$ approaches 0. Comparing these results with the previous comparisons between the x-ray and OIM textures indicates that approximately 20 to 1300 measurements (depending on the scan) are needed to achieve the same agreement (0.5) as that obtained

for the forged copper. The sharper textures (*Fiber Al* and *Ta Plate*) require fewer measurements to reach the desired accuracy.

Instead of considering the number of measurements needed for statistical accuracy it is also useful to consider the sampling area needed to accurately determine an OD. To examine this question, a circle of radius R was placed at a random position within the area defined by the OIM scan. An OD was calculated using all of the measurements from the scan lying within the prescribed circle. The value D_R^N was then calculated for the OD obtained from the point lying within the circle (denoted R) and the OD calculated from all of the measurements in the data set (denoted by the N). This was done for ten circles of radius R and the average D_R^N value calculated. This procedure was repeated for several radii and an average D_R^N calculated. The results are plotted as a function of R, normalized by the average grain diameter (d) in Fig 9.

In OIM the term "grain" has a very specific meaning. For each point on the OIM scan grid, the neighbors are checked to see if they are within a user specified angle in orientation of the particular point. If a neighboring point is within the specified tolerance angle then its neighbors are checked to see if they meet this criterion. The procedure is repeated again and again until the set of connected points is bounded by points which exceed the tolerance angle. Using this approach, the point-to-point misorientations in the "grain" will be quite small, but the spread in orientation among all points in the grain can be relatively large. The area of such a grain formed using OIM is equal to the array spacing times the number of points in the grain multiplied by the factor $\sqrt{3}/2$ to account for the hexagonal grid. The grain diameter for such a "grain" is then given by $d = (4A/\pi)^{1/2}$, where A is the area encompassed by the "grain".

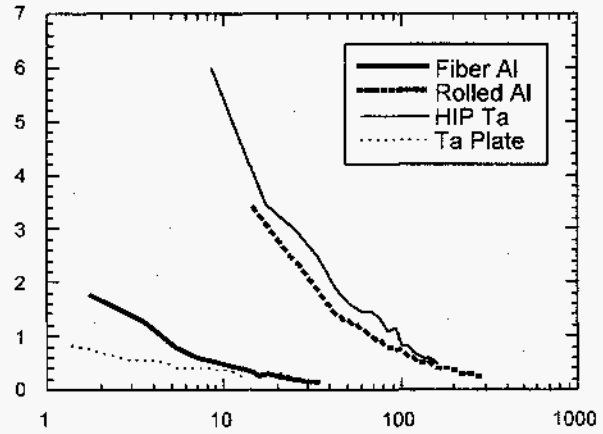

Fig. 9 Plot of D_R^N versus R/d (d is the average grain diameter).

These results indicate that less measurements and a smaller sampling area are needed for sharp textures as opposed to more random textures.

DISCUSSION AND CONCLUSIONS

The differences observed between the x-ray and OIM textures may appear at first glance to be negligible. However, the examples presented show the danger of using a single scalar parameter to describe the difference between two ODs. Such a parameter may indicate that two textures are quite similar. However, there may be distinct differences at very key locations in Euler space (such as cube) which may vary substantially, even though, the overall error may be quite small.

In general, the primary differences observed in these results are in the heights and shapes of the main peaks in the texture. However, these types of differences can often be reduced by adjusting some of the calculation parameters used in reducing the data. It should be noted that when volume fractions are calculated for these peaks the same result may be obtained depending on the spread used to calculate the volume fraction. Volume fractions have been traditionally calculated by integrating the OD over a specific region in Euler space. For OIM data, the volume fraction can be calculated by counting the number of orientation measurements within the specified range of the peak position and then dividing this number by the total number of measurements in the data set.

Although, the main differences observed in this study were generally associated with major peaks in the orientation distribution; in terms of properties predictions, the more subtle differences associated with less conspicuous features in the texture may be of more concern. These more subtle differences may have significant effects on the prediction of properties such as yield behavior [13].

The differences observed in this study are similar to those observed in the neutron diffraction standard experiment carried out by Wenk [17]. Several institutions measured the texture of a standard polycrystalline specimen by neutron diffraction. In general, the pole figures obtained from the different institutions were all quite similar. However, there were noticeable differences and these differences seem to have been on the same scale as those observed in this study.

The pole figure deconvolution methods do not appear to be responsible for the deviations observed in this study. There was no reason to suspect that the absence of the odd-l terms was responsible for the differences in the rolled copper example and for the fiber textures the odd-l ambiguity does not exist.

It is difficult to state for the textures presented here whether the x-ray textures or the OIM textures are "correct". It should be remembered that electron diffraction is a point sampling measurement technique, x-ray diffraction is a surface area technique and neutron diffraction a bulk volume sampling technique. (However, with the mapping of the orientations across the surface of a sample using the automated OIM technique it is also possible to consider electron diffraction as an area sampling technique). Thus, for bulk properties neutron diffraction should offer the most reliable texture measurement. Neutron diffraction measurements are planned to complete the comparisons presented here.

ACKNOWLEDGEMENTS

The authors are appreciative of C. T. Necker of Los Alamos National Lab for providing the data on the rolled copper. We also acknowledge G. T. Gray III for providing the copper cone sample and S. R. Bingert and A. M. Kelley for help with the tantalum samples. This work was performed under the auspices of the United States Department of Energy. OIM is a trademark of TexSEM Laboratories, Inc., Provo, Utah.

REFERENCES

1. B.L. Adams, S.I. Wright & K. Kunze, Met. Mat. Trans.
2. S.I. Wright, J. Computer Assisted Microscopy,
3. S. Matthies, Physica status solid, 92(1979) K135
4. K. Lücke, J. Pospiech, K.H. Virnich & J. Jura, Acta Met., 29 (1981), 167.
5. M. Dahms & H.J. Bunge, Proc. Eighth Int. Conf. On Textures of Materials, edited by J.S. Kallend & G.Gottstein, 1987, p. 79, Warrendale, PA: Metallurgical Society.

6. A. Bowen, Materials Science Forum, 157-162 (1994), 315.
7. S. I. Wright & B.L. Adams, Textures and Microstructures, 12 (1990), 65.
8. T. Baudin & R. Penelle, Mat. Trans. 24A (1993), 2299.
9. O. Engler, P. Yang, G. Gottstein, J. Jura & J. Pospiech, Materials Science Forum, 157-162 (1994), 993.
10. Y.S. Liu, R. Penelle, F. Wang, J.Z. Xu & Z.D. Liang, Materials Science Forum, 157-162 (1994), 375.
11. J.S. Kallend, U.F. Kocks, A.D. Rollett & H.-R. Wenk, Mat. Sci. Eng., A132 (1991), 1.
12. U.F. Kocks, Proc. Eighth Int. Conf. On Textures of Materials, edited by J.S. Kallend & G.Gottstein, 1987, p. 31, Warrendale, PA: Metallurgical Society.
13. U.F. Kocks, S.I. Wright & A.J. Beaudoin, These proceedings.
14. P.A. Hollinshead, Aluminum Alloys for Packaging II, edited by J.G. Morris, S.K. Das & H.S. Goodrich, 1996, p. 117, Warrendale, PA: The Minerals, Metals & Materials Society.
15. S.I. Wright, G.T. Gray III & A.D. Rollett, Met. Mat. Trans., 25A (1994), 1025.
16. J.B. Clark, R.K. Garrett, Jr., T.L. Jungling, R.A. Vandermeer & C.L. Vold, Met. Trans, 22A (1991), 2039.
17. H.-R. Wenk, J. Appl. Cryst., 24 (1991), 920.
18. S.I. Wright, A.D. Rollett & M.G. Stout, Scripta Met. Mat., 28 (1993) 985.